

Article

Automatic Control System for Maize Threshing Concave Clearance Based on Entrainment Loss Monitoring

Yang Yu ^{1,2} , Yi Cheng ³, Chenlong Fan ^{4,*} , Liyuan Chen ¹, Qin hao Wu ¹, Mengmeng Qiao ⁴ and Xin Zhou ²

¹ College of Agricultural Engineering, Jiangsu University, Zhenjiang 212013, China; yu_yang@ujs.edu.cn (Y.Y.); 2112216005@stmail.ujs.edu.cn (L.C.); 2212352002@stmail.ujs.edu.cn (Q.W.)

² Key Laboratory for Theory and Technology of Intelligent Agricultural Machinery and Equipment, Jiangsu University, Zhenjiang 212013, China; zhouxin_21@ujs.edu.cn

³ Changzhou Changfa Heavy Industry Technology Co., Ltd., Changzhou 213167, China; chengyi709@126.com

⁴ College of Mechanical and Electronic Engineering, Nanjing Forestry University, Nanjing 210037, China; qiaomengmeng2024@njfu.edu.cn

* Correspondence: fancl@njfu.edu.cn

Abstract: Complex harvesting environments and varying crop conditions often lead to threshing cylinder blockage and increased entrainment loss in maize grain harvesters. To address these issues, an electric-driven automatic control system for maize threshing concave clearance based on real-time entrainment loss monitoring was developed. The system automatically adjusts concave clearance parameters at different harvesting speeds to maintain grain entrainment loss within an optimal range. First, an adjustable concave structure based on a crank-link mechanism was designed, with a threshing clearance adjustment range of 15–47 mm and motor rotation angle of 0–48°. Subsequently, an EDEM simulation model of the mixed material discharge inside the threshing cylinder was established to determine the optimal installation position of the entrainment loss monitoring sensor based on piezoelectric ceramic-sensitive elements. The sensor was positioned at the left tail end of the concave sieve, with a minimum distance of 58 mm between the sensitive plate centerline and threshing concave sieve and an installation angle of 65° relative to the horizontal plane. A maize threshing clearance control method based on fuzzy neural network PID control algorithm was proposed, and Simulink simulation optimization verified its superior performance with fast response speed. After system integration, field trials were conducted at low, medium, and high operating speeds with preset ideal entrainment loss intervals. The results showed that control was unnecessary at low speed, the control system-maintained entrainment loss within set range at medium speed, and maximum threshing clearance was needed at high speed. Finally, comparative trials of threshing performance with and without the control system were conducted at medium harvesting speed. Results showed that the entrainment loss rate decreased by 43.75% with the control system activated, significantly reducing maize threshing entrainment losses. This study overcame the barrier of maize threshing parameter adjustment being heavily reliant on manual experience and provided theoretical support for the intelligent grain harvesting equipment.

Keywords: maize harvester; threshing cylinder; concave clearance; entrainment loss; automatic control system



Academic Editor: Olympia Roeva

Received: 3 December 2024

Revised: 19 December 2024

Accepted: 27 December 2024

Published: 30 December 2024

Citation: Yu, Y.; Cheng, Y.; Fan, C.; Chen, L.; Wu, Q.; Qiao, M.; Zhou, X. Automatic Control System for Maize Threshing Concave Clearance Based on Entrainment Loss Monitoring.

Processes **2025**, *13*, 58. <https://doi.org/10.3390/pr13010058>

Copyright: © 2024 by the authors.

Licensee MDPI, Basel, Switzerland.

This article is an open access article distributed under the terms and conditions of the Creative Commons

Attribution (CC BY) license

(<https://creativecommons.org/licenses/by/4.0/>).

1. Introduction

Maize is an important crop that can be processed into various food and industrial products such as starch, sweeteners, beverages, glue, industrial alcohol, and fuel ethanol [1–3].

In 2023, China's maize planting area was approximately 44.22 million hectares, making it one of the world's largest maize producers and consumers [4–6]. Maize harvesting is typically conducted when the grain moisture content is between 20 and 35%, followed by extended drying until the moisture content reaches around 15% before threshing with small threshers [7,8]. This method has disadvantages, including long processing cycles, high labor intensity, and high operating costs, which cannot meet modern maize production requirements [9,10]. Therefore, China's maize harvesting operations are gradually transitioning to direct grain harvesting, which is significant for shortening harvest cycles, saving production costs, improving operational efficiency, and promoting agricultural mechanization.

The threshing device is a crucial component for direct harvesting of maize grain [11–13]. When maize kernels enter the threshing chamber, they are separated from the cob through impact, collision, and kneading [14]. The structural design and operating parameters of the threshing device directly affect the grain entrainment loss rate and breakage rate [15,16]. Currently, operations mainly rely on operators' sensory perception and experience, leading to performance fluctuations that vary by operator [17–19]. Therefore, research on automatic control of threshing devices is extremely important. Domestic and international scholars and agricultural machinery enterprises have conducted extensive research and experiments on threshing and cleaning intelligence over the past two decades. Currently, only a few Chinese brands (such as Lovol Guoshen GK120, World Dragon, etc.) are equipped with simple information functions like multi-channel speed monitoring and blockage alarms for threshing and cleaning components, generally lacking intelligent control technology [20]. Advanced agricultural machinery companies from Europe and America, such as JOHN DEERE, CLAAS, and CNH, have widely applied real-time monitoring of operational performance and intelligent control technologies in their grain combine harvesters, achieving adaptive adjustment of working parameters such as threshing cylinder speed, sieve box inclination, and sieve opening. However, their sensors for monitoring losses, impurities, and breakage, as well as performance control systems, are not well-suited to Chinese crop varieties, lack universality, and their core technological equipment is restricted to China [21,22]. In 2010, Omid et al. [23] designed a fuzzy logic controller (FLC) based on expert knowledge, achieving automatic control of the combine harvester's threshing cylinder speed, concave clearance, fan speed, and forward speed based on real-time monitoring of entrainment and sieve losses to minimize grain losses. In 2015, AGCO Corporation invented a constant-pressure concave sieve for combine harvesters that adjusts concave clearance by automatically controlling hydraulic cylinder piston rod extension to maintain optimal threshing load and prevent blockage. In 2015, Ning Xiaobo et al. [24] established a dynamic model of the threshing system and combined it with a fuzzy logic controller to build a cylinder speed control system simulation model to avoid cylinder overload or blockage. In 2018, Zhang et al. [25] proposed a threshing separation quality control strategy based on fuzzy logic, using concave clearance and cylinder speed as inputs in a dual input-single output two-dimensional Mamdani-type fuzzy controller structure to control threshing separation quality, with objectives of low loss rate and low breakage rate. In 2020, Lian [26] proposed an inference method for grain entrainment loss, breakage, and impurity rate based on BP neural network technology, using monitoring data of concave clearance, cylinder speed, and forward speed to predict multi-operational parameters of the threshing device. In 2022, Zhu et al. [27] designed a low-loss threshing intelligent control system simulation platform for developing harvester intelligent control systems and testing control strategies, improving system development efficiency and shortening development cycles. The above threshing device control system achievements are mainly in paper form and still some distance from actual productization [28]. Furthermore, input

feedback conditions in existing threshing parameter control model research mostly come from calculated values, lacking accurate sensors for monitoring operational performance such as losses, impurities, and breakage, resulting in unsatisfactory control system effects in actual harvesting operations and low robustness.

To enhance the accuracy and robustness of the parameter control system for maize threshing, the fuzzy control method demonstrates significant advantages in the field of maize harvesting. It enables precise control of complex nonlinear systems, particularly in scenarios where environmental variables are highly variable during mechanical operations and where it is difficult to establish precise models. By introducing fuzzy control, the system can dynamically adapt based on real-time monitoring parameters (such as threshing gap, drum speed, and grain loss rate) without relying on an accurate mathematical model. Compared with traditional PID control, fuzzy PID control exhibits stronger robustness and adaptability, effectively reducing delays and instabilities in machinery parameter adjustments, thereby lowering both loss rates and grain breakage rates. It enhances harvesting efficiency and quality, providing a reliable guarantee for the automation and performance optimization of maize harvesting machinery.

Therefore, to address the issues of monitoring and adjusting the operational performance of advanced harvesting equipment imported from abroad, which cannot adapt to Chinese crop varieties, this paper focuses on the mechanical harvesting of Chinese maize varieties and innovatively proposes an automatic control method for the threshing concave clearance of maize combine harvesters based on entrainment loss monitoring. The rest of the paper is arranged as follows: Section 2 provides a detailed introduction to the mechanical structure of the electric control adjustment device for the threshing concave clearance, the adjustment system, the installation position of the entrainment loss sensor, and the system simulation results based on entrainment loss monitoring and fuzzy PID control. Field experimental results and discussions are provided in Section 3, discussing the impact of different operational speeds on the control performance of entrainment loss and the comparative results of threshing performance before and after the control system was activated.

2. Materials and Methods

2.1. Electric Control Adjustment Device for Threshing Clearance

Threshing clearance refers to the gap between the cylinder threshing elements and the concave surface. This clearance plays a crucial role in the combined harvester's operational performance. The electric control adjustment device for threshing clearance designed in this paper is shown in Figure 1, comprising an adjustable threshing lower sieve, stepper motor, rotating shaft, connecting arm, displacement sensor, etc. The adjustment device structure uses a crank-rocker mechanism design, converting the axial rotational motion from the stepper motor output end into threshing clearance changes through connecting arms and various pins and shafts.

As shown in Figure 1, one side of the concave is connected via suspension, while the other side is hinged to the turning arm of the threshing clearance adjustment mechanism. The hydraulic cylinder's motion causes the crank to rotate, making the push rod move up and down, adjusting the concave up and down. During threshing, maize ears move counterclockwise with the threshing rotor. To prevent damage to the actuator when reaching limit positions in special circumstances, the crank-link mechanism's limit positions are calibrated. When the motor rotation angle is between 0 and 48°, the threshing clearance adjustment range is 15–47 mm. The threshing clearance can be adjusted according to the motor's rotation angle—the larger the motor rotation angle; the greater the threshing clearance adjustment.

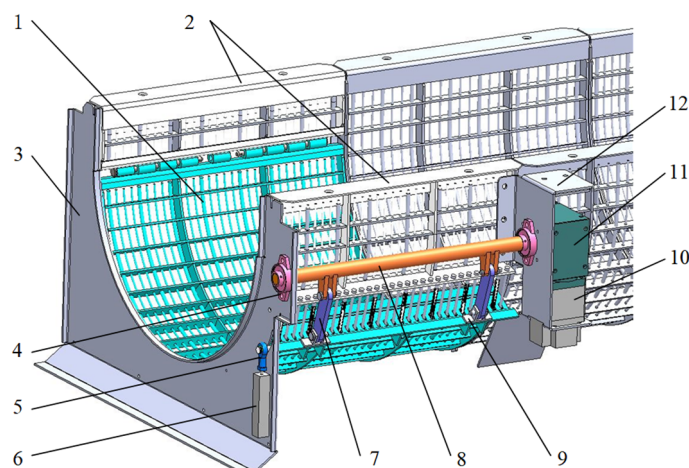


Figure 1. Adjustable threshing concave sieve, (1) adjustable lower threshing screen; (2) fixed upper threshing screen; (3) drum inlet baffle; (4) bearing seat; (5) rod end joint bearing; (6) displacement sensor; (7) connecting arm; (8) rotating shaft; (9) connecting ear; (10) stepper motor; (11) gearbox; (12) mounting bracket.

2.2. Threshing Clearance Control System Architecture

The automatic control system for threshing clearance mainly consists of threshing separation devices, electric control threshing clearance adjustment mechanisms, grain entrainment loss monitoring devices, and controller units, with the overall system architecture shown in Figure 2. The grain entrainment loss monitoring device is located below the tail end of the threshing concave sieve, collecting maize grain entrainment loss count and outputting it to the controller to guide automatic threshing clearance adjustment. Through the crank-link mechanism, the axial rotational motion from the stepper motor output end is converted into threshing clearance changes.

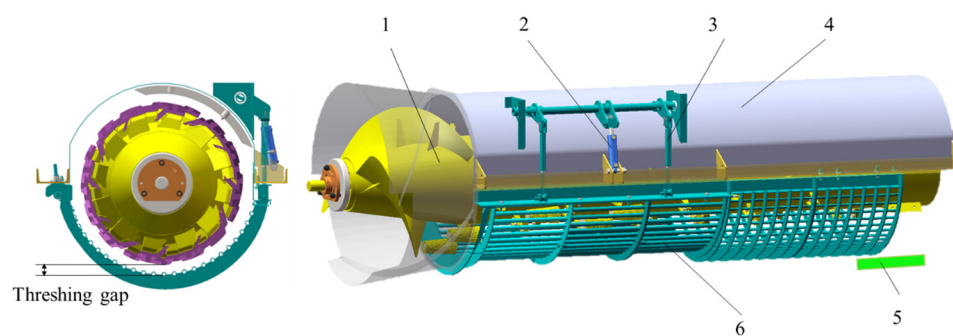


Figure 2. Control System Architecture. 1. Rotor 2. Hydraulic cylinder 3. Crank of threshing gap adjustment mechanism 4. Cover plate 5. Piezoelectric loss sensor 6. Threshed concave.

The stepper motor selected for the threshing clearance electric control adjustment device is the Z5BLD120-24 from Zhongda Lide Company (Ningbo, China), with an RV050 worm gear reducer from Bilin Hardware and Electric Company (Hangzhou, China). Through force analysis and calculation, the reducer output end's torque and speed can meet the requirements for threshing clearance adjustment torque, stroke, and control response speed. The stepper motor is equipped with a ZBLD.C20-400LR type driver, and the threshing clearance measurement feedback device uses a KTC1-75 mm type from Milang Company (Shenzhen, China), with a monitoring error of less than 0.1%.

2.3. Real-Time Entrainment Loss Monitoring and Result Calibration

2.3.1. Loss Monitoring Sensor Installation Position

The entrainment loss monitoring sensor is developed based on piezoelectric principles. To reduce the sensor's blocking effect on falling mixed material, each monitoring sensor's sensitive plate dimensions are 150 mm (length) \times 120 mm (width), with an effective monitoring area of 17,867 mm². The sensitive plate is made of 304 stainless steel with a 1 mm thickness. PZT-5 type piezoelectric ceramics are adhered to symmetrical positions on the back center of the sensitive plate, with dimensions and thickness the same as the previously mentioned piezoelectric ceramics.

Based on the threshing separation probability model of the axial-flow cylinder, the structure and installation position of the entrainment loss monitoring sensor were designed and determined, as shown in Figure 3. The sensor is located below the rear end of the threshing concave sieve and mounted on the inner wall of the threshing device, avoiding the impact of large amounts of long stalks at the straw discharge outlet. The material baffle is positioned above the sensitive plate to prevent the accumulation of a threshed mixture between the sensitive plate and the inner wall of the threshing device. The minimum distance between the centerline on the sensitive plate and the threshing concave sieve is 58 mm, and the installation angle of the sensor relative to the horizontal plane is 65°. Through previous research team's calibration experiments on maize threshing impact signals [22], it was determined that bandpass filtering frequency of 14–20 kHz can accurately identify grain kernels.

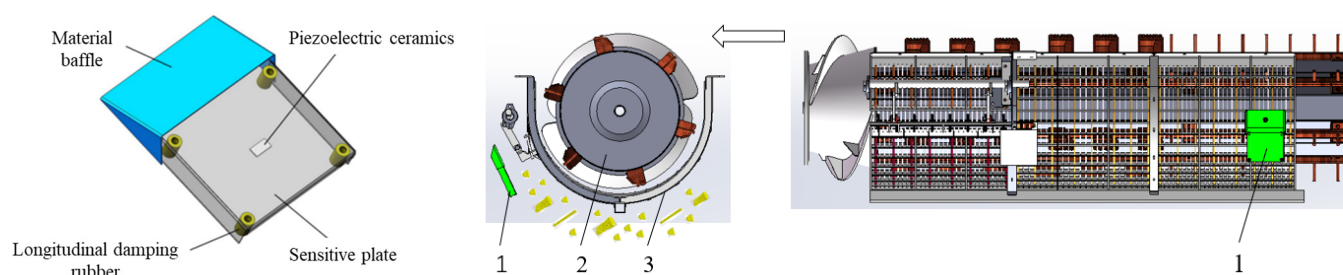


Figure 3. Structural and Installation Position of Entrainment Loss Monitoring Sensor. 1. Entrainment Loss Sensor 2. Threshing Cylinder 3. Separation Concave Sieve.

2.3.2. Simulation of Entrainment Loss Monitoring Process

To obtain the actual number of entrained grain kernels during the threshing process, it is necessary to establish a mathematical relationship between the monitored and actual entrainment loss values. This paper uses DEM (Discrete Element Method) simulation to study the actual distribution pattern of entrainment loss, investigate the variation in the proportion of sensor-monitored losses to actual losses under various working conditions, and perform parameter correction of the monitoring system to further improve the monitoring accuracy of the loss sensor.

(1) Simulation Model Establishment and Parameter Settings

Based on the three-dimensional model of the full-ribbed threshing cylinder designed in SOLIDWORKS software (length 1900 mm, total width 930 mm, total height 714 mm), including the closed threshing cylinder shell, threshing elements, threshing concave sieve, threshing cylinder sidewall, top cover guide plate, entrainment loss monitoring sensor, and other structures, it was imported into the EDEM simulation model. Threshing operation simulation was conducted by manually setting varying feed rates.

In the EDEM simulation model, the gravity acceleration direction was set perpendicular to the top cover of the threshing device, with a magnitude of 9.81 m/s². The threshing

cylinder speed was set to the rated condition of 700 r/min, with rotation axis and direction specified. The three-dimensional dimensions and mechanical property parameters of various particle models in the threshing device mixture are shown in Figure 4 and Table 1. During actual harvesting, crops in the threshing device may deform or break, and kernels may separate from the ear, but these processes are difficult to simulate in EDEM software. Therefore, to simplify the simulation process, stalks in the threshing device were set as rigid bodies, and kernels were set as discrete bodies after separation. The Bonding model was used for discrete element simulation, with a calculation time step of 0.000002 s and a total simulation duration of 4.8 s.

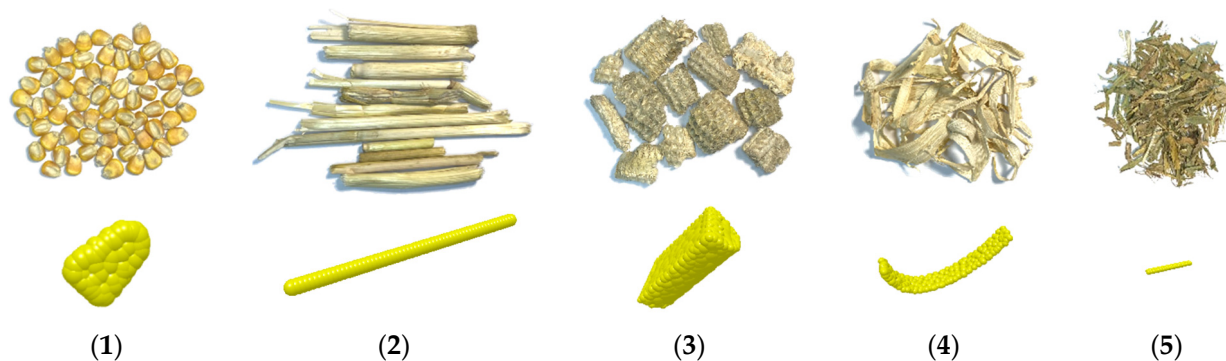


Figure 4. Maize threshing mixture particle models: (1) grain kernels; (2) short stalks; (3) maize cobs; (4) maize leaves; (5) light residue.

Table 1. Three-dimensional Mechanical Property Parameters of Maize Particle Models.

Parameters	Maize Kernels	Short Stalks	Maize Cobs	Maize Leaves	Light Residue
Length × Width × Thickness/mm	9.1 × 6.2 × 2.5	63.2 × 3.7 × 3.7	40.1 × 21.7 × 15.9	83.0 × 26.2 × 1.0	10.9 × 1.5 × 0.8
Density/kg·m ⁻³	1180	112	421	88	75
Poisson's Ratio	0.4	0.4	0.5	0.4	0.4
Shear Modulus/Pa	9.8 × 10 ⁷	7.5 × 10 ⁶	4.7 × 10 ⁶	1.8 × 10 ⁶	2.0 × 10 ⁶

(2) Calibration of Entrainment Loss Monitoring Ratio

The DEM simulation results of the proposed maize threshing device under maximum feed rate and 28 mm threshing clearance conditions are shown in Figure 5. In the simulation diagram, the different colored particles represent different organs of the maize plant: yellow represents maize kernels, green represents short stalks, red represents long stalks, cyan represents light contaminants, magenta represents maize cobs, and light green represents maize leaves.

- ① At $t = 0.6$ s, the mixture is mainly concentrated in the front-middle part of the threshing device. Some mixture components, such as short stalks and light residue, have already moved to the device outlet, while most kernels and some short stalks and light residue pass through the threshing concave sieve and fall.
- ② At $t = 1.8$ s, the mixture fills the entire threshing device. A small portion of kernels and most short stalks, long stalks, and light residue are discharged from the device outlet. Most kernels and some short stalks and light residue pass through the threshing concave sieve and fall. Some kernels impacting the entrainment loss monitoring sensor constitute the monitored loss, while kernels discharged through the device outlet cannot be monitored.
- ③ At $t = 4.8$ s, the degree of mixture filling, discharge rate, and sieve passage show little difference compared to $t = 1.8$ s, indicating that mixture movement has reached a relatively stable state during $t = 1.8$ s to $t = 4.8$ s. Therefore, this

time period is selected as the optimal phase for analyzing the monitoring ratio data of the entrainment loss sensor.

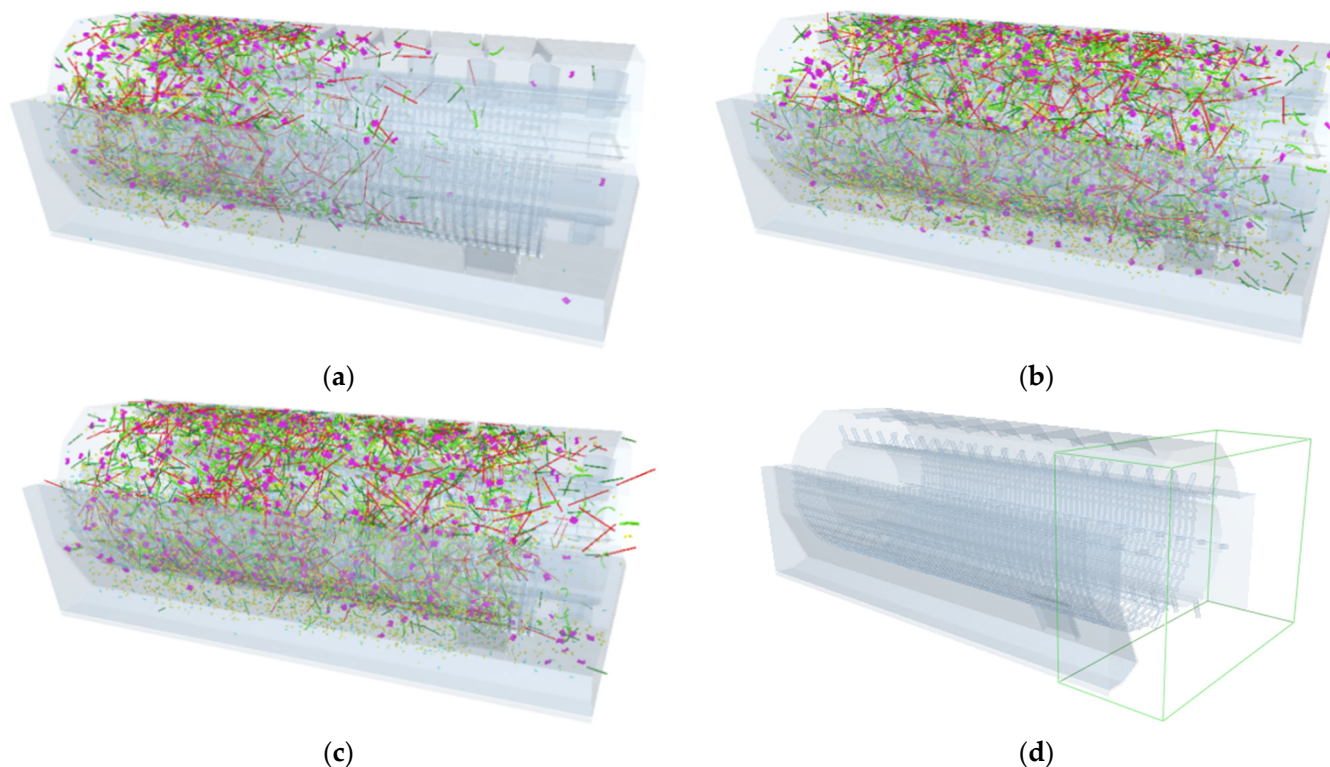


Figure 5. Maize threshing device simulation, (a) $t = 0.6$ s; (b) $t = 1.8$ s; (c) $t = 4.8$ s; (d) total entrainment loss counting area (green frame).

After completing the simulation calculations, a particle counting region was created in the EDEM software analysis interface (Figure 5d) to count all grain particle models discharged from the rear of the threshing device. From the EDEM software output data, the number of kernels colliding with the entrainment loss monitoring sensor and the number of kernels in the total entrainment loss counting area during the period $t = 1.8$ s to $t = 4.8$ s were exported. The entrainment loss monitoring ratio was obtained by dividing these two values. Through field feeding trials studying the influence of threshing clearance on monitoring ratios, the following values were obtained (Table 2):

Table 2. Entrainment Loss Monitoring Ratio Values.

Threshing Clearance Range/mm	Maize Entrainment Loss Monitoring Ratio/%
[14, 21]	10.8
[21, 28]	11.5
(28, 36]	12.3

2.4. Automatic Threshing Clearance Control System

2.4.1. Fuzzy Neural Network PID-Based Threshing Clearance Control System

The automatic threshing clearance control system forms a closed-loop control through the entrainment loss sensor, control board, power supply, speed controller, driver, actuator, and displacement sensor. The main function of the control board is to process information collected by the entrainment loss sensor, output adjusted linear displacement sensor signals, and issue commands to drive the speed controller and actuator, thereby forming a closed-loop system. Figure 6 is the control flowchart.

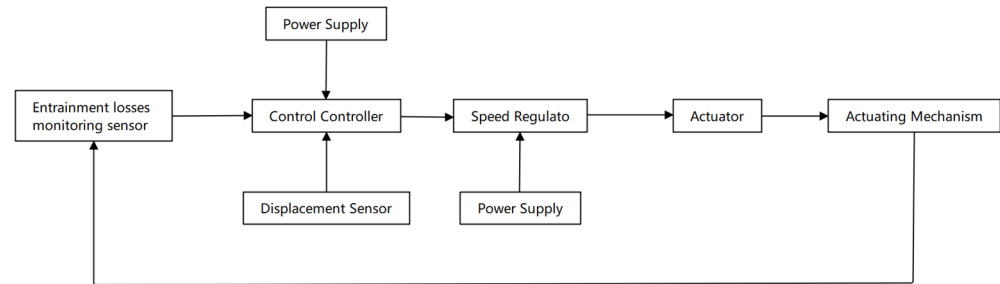


Figure 6. The control system flowchart.

To achieve optimal threshing effects with real-time parameter updates under complex harvesting conditions, this paper proposes a threshing clearance control method based on fuzzy neural network PID. The fuzzy neural network PID control system combines the advantages of conventional PID control, fuzzy control, and neural networks, improving system speed and accuracy to effectively solve control system oscillation, delay, and other issues [27].

With the goal of maintaining the entrainment loss rate within the optimal range, a fuzzy neural network PID system is established using the entrainment loss monitoring value and its deviation e from the ideal range, along with the rate of deviation change ec as inputs and the threshing gap value as output. Each node in the input layer of the fuzzy neural network is represented as [29]:

$$net_1(i) = X = [x_1 \ x_2 \ \dots \ x_n] \quad (1)$$

In the Equation, x_1 represents the deviation, and x_2 represents the rate of change of the deviation. A Gaussian radial basis function is used as the membership function, where c_{ij} and b_{ij} are the center and width of the membership function for the i -th input variable and j -th fuzzy set, respectively [30].

$$net_1(i, j) = e^{-\frac{(net_1(i) - c_{ij})^2}{b_{ij}^2}} \quad (2)$$

The product of the input signals is used to represent the output of node j in the fuzzy inference layer:

$$net_3(j) = \prod_{i=1}^N net_2(i, j) \quad (3)$$

The fuzzy inference layer, together with the weighted sum of their respective weights, represents the output layer [29]:

$$net_4(j) = w * net_3 = \sum_{i=1}^N w(i, j) * net_3(j) \quad (4)$$

The controller [31]:

$$\Delta u(k) = k_p xc(1) + k_i xc(2) + k_d xc(3) \quad (5)$$

$$xc(1) = e(k) \quad (6)$$

$$xc(2) = e(k) - e(k-1) \quad (7)$$

$$xc(3) = \Delta^2 e(k) = e(k) - 2e(k-1) + e(k-2) \quad (8)$$

The incremental PID control algorithm is adopted [28]:

$$u(k) = u(k-1) + \Delta u(k) \quad (9)$$

The Delta learning rule is used to adjust the tunable parameters, with the objective function defined as:

$$E = \frac{1}{2}(rin(k) - yout(k))^2 \quad (10)$$

In the Equation, $rin(k)$ and $yout(k)$ represent the actual measured value and the ideal reference value, respectively. The control error at step k is defined as $e(k) = rin(k) - yout(k)$.

The calculation of network weights is as follows [29]:

$$\Delta w_j(k) = -\eta \frac{\partial E}{\partial w_j} = -\eta * e(k) * net_3(j) \quad (11)$$

The calculation of the center vector in the fuzzification layer is as follows:

$$\Delta b_j(k) = -\eta \frac{\partial E}{\partial b_j} = -\eta * e(k) * 2 * net_3(j) * \frac{(x_j - c_{ij})^2}{b_j^3} \quad (12)$$

The calculation of the basis width vector in the fuzzification layer is as follows:

$$\Delta c_{ij}(k) = -\eta \frac{\partial E}{\partial c_{ij}} = -\eta * e(k) * 2 * w_j(k) * \frac{(x_j - c_{ij})^2}{b_j^2} \quad (13)$$

Under the influence of the momentum factor, the weights of the output layer are calculated as:

$$w_j(k) = w_j(k-1) + \Delta w_j(k) + \alpha(w_j(k-1) - w_j(k-2)) \quad (14)$$

The Equation indicates that k represents the iteration step and α is the momentum factor.

In this study, a quantification table of entrainment loss prediction deviations and their changes is used to determine the corresponding quantization levels and fuzzification metrics. The fuzzification of inputs and outputs is based on the calculation of entrainment loss and the ideal threshold. The basic range of entrainment loss deviation and its variation is derived from calibration tests, indicating that the optimal number of entrained loss grains to monitor is 14–28 g/s (with the ideal loss rate set between 0.5% and 1%). Any intermediate value within this range can be chosen as the reference value.

To discretize the basic domain into a finite set of values, a fuzzy domain is defined as $e = ec = \{-3, -2, -1, 0, 1, 2, 3\}$. Each fuzzy level corresponds to a specific range of change as listed in Table 3.

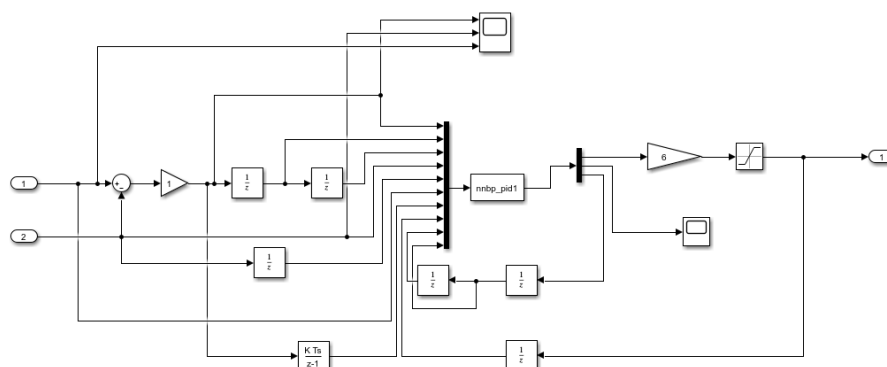
The number of entrained grain losses during threshing is set using fuzzy quantization, divided into 7 levels. The optimal zero point for grain losses is set in the range of 14–28 grains. The control system automatically adjusts the actuators, allowing the threshing concave clearance to dynamically adapt to changes in entrained losses, thereby maintaining the loss rate within the optimal range. The loss rate during threshing and the threshing concave clearance are negatively correlated. Therefore, to reduce entrained losses, the threshing concave clearance must be increased. To keep entrained losses within the ideal range, the threshing concave clearance must be decreased. The extent of threshing concave clearance adjustment is represented by the output of a displacement sensor, with a basic adjustment range of ± 10 mm.

Table 3. Quantitative table of threshing deviation e and deviation change rate ec .

Quantization Level	e Change Range	ec Change Range
-3	<-14	<-10
-2	-14~-11	-10~-7
-1	-11~-7	-7~-4
0	-7~7	-4~4
1	7~17	4~10
2	17~28	10~15
3	>28	>20

2.4.2. Simulation Analysis of Threshing Gap Control System

To evaluate the effectiveness and robustness of the assembled fuzzy neural network PID controller, MATLAB software (R2021a) was used for modeling and Simulink simulation of the control process, thereby adjusting system parameters and improving the model structure. Simulink, a visual simulation tool within MATLAB, offers advantages such as a wide range of adaptability, clear structure and flow, high fidelity and realism in simulations, efficiency, and flexibility. It has been widely used in complex simulations and designs in control theory and digital signal processing. The loss data obtained from the filtered real-time monitoring signals of the entrainment loss sensor, along with the motion data of the actuator monitored by the linear displacement sensor, are input into the multiplexer and then processed by the fuzzy neural network PID controller to ultimately output the desired value of threshing concave clearance. The structural diagram of the fuzzy neural network PID simulation program is shown in Figure 7.

**Figure 7.** Fuzzy Neural Network PID Controller Model.

In the simulation model, the output is the threshing concave clearance displacement signal. The purpose of adding a limit is to protect the actuator's movement within a safe range, restricting the minimum and maximum stroke of the actuator. The loss grain value is set at 35 (entrainment loss rate of 1.2%) and controlled by the system to reach 18 (entrainment loss rate of 0.7%).

3. Results and Analysis

3.1. Field Trial Design

To verify the performance of the maize threshing gap control system based on fuzzy PID, using entrainment loss rate as the evaluation index, the working performance of the control system at different harvesting speeds was compared. Through field trial results, the entrainment loss rates before and after the control system activation were analyzed to verify the effectiveness of the control system. The maize field harvesting trials were conducted from 20 to 24 October 2024, in Erlangmiao Village, Da'an Town, Yanzhou District, Jining City, Shandong Province. Some maize material characteristics are shown in Table 4.

Table 4. Maize Material Characteristics.

Parameter	Value
Maize variety	958
Yield per mu (kg)	863.55
Plant height (cm)	232.73
Ear height (cm)	118.31
1000-g weight (g)	355.22
Plant spacing (mm)	250.56
Moisture content (%)	22.67
Main stem diameter (mm)	31.72

During the field trials, the maize threshing gap control system was activated, and the ideal range for entrainment loss was set. The maize harvester was operated at different forward speeds for multiple harvest trials. During each harvesting process, the loss rate monitored by the entrainment loss sensor and the displacement sensor output were recorded under stable operating conditions.

3.2. Impact of Different Operating Speeds on Entrainment Loss Control Performance

Operators typically harvest at three speeds: low, medium, and high. This study similarly selected three different constant speeds of 0.5 m/s, 1 m/s, and 1.5 m/s for maize grain harvesting trials. In each trial group, the control program was activated after the harvester had been operating for 20 s and reached a stable harvesting phase.

The trend lines of maize grain loss and gap adjustment under different forward speeds are shown in Figure 8, with the optimal loss grain count range set between an upper limit of 28 g and a lower limit of 14 g. The control system remained inactive for the first 20 s with a constant threshing gap and was activated after 20 s. Within 0–10 s, the harvester’s main working components reached a stable state. The grain loss trend line during normal harvesting conditions can be observed during 10–20 s, while the regulated grain loss trend line is visible after 20 s.

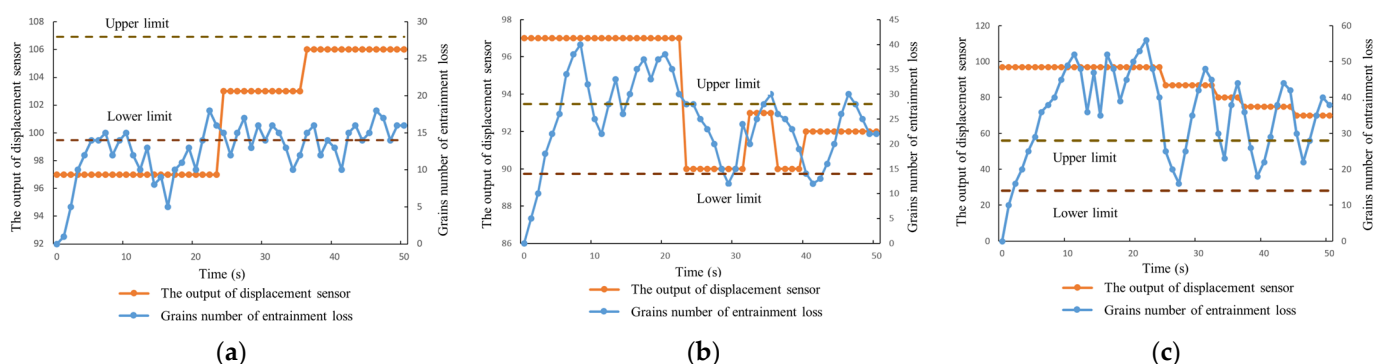


Figure 8. Trend lines of entrainment loss regulation with different driving speeds. (a). 0.5 m/s; (b) 1.0 m/s; (c) 1.5 m/s.

From the grain loss trend line in Figure 8a, when the forward speed was maintained at 0.5 m/s, the entrainment loss grain count stabilized between 10 and 15 g/s during the first 20 s. After 20 s, when the entrainment loss grain count fell below the ideal value of 14, the displacement output began to increase, and the threshing gap decreased. The loss value remained within the ideal range for the majority of the time, indicating low entrainment loss during low-speed operation [32,33]. Therefore, automatic threshing gap control is unnecessary at lower forward speeds.

From the grain loss trend line in Figure 8b, when the forward speed was maintained at 1 m/s, the entrainment loss grain count fluctuated between 10 and 40 g/s during the first 20 s, showing significant variations. After activating the control system at 20 s, the entrainment stabilized between 12 and 30 g/s, with an average loss of 21 g/s, showing reduced grain loss fluctuation within the ideal range. When the loss fell below 14, indicating low loss, the displacement output increased and the threshing gap decreased; when it exceeded 28, indicating high loss, the displacement output decreased and the threshing gap increased.

From the control trend line in Figure 8c, when the forward speed was maintained at 1.5 m/s, the entrainment loss grain count stabilized between 20 and 50 g/s during the first 20 s and between 23 and 50 g/s from 20 to 50 s, with entrainment loss mostly exceeding the ideal range. Therefore, during high-speed field operations, the threshing gap should be set to maximum to reduce entrainment loss.

In summary, the comparison of entrainment loss before and after control implementation at three different forward speeds demonstrates that increased forward speed leads to increased entrainment loss. Therefore, the control system is unnecessary at lower forward speeds; at medium speeds, activating the control maintains entrainment loss within the set range; and at high forward speeds, the threshing gap should be maximized to reduce entrainment loss.

3.3. Comparison of Threshing Performance Before and After the Control System Is Activated

To verify the performance of the threshing gap control system, manual collection of the carryover loss amount was conducted before and after the control system was activated (Figure 9). Given the superior adjustment performance of maize harvesting at medium-speed operations, a working speed of 0.8–1.3 m/s was adopted. Before the experiment, a testing area of 30 m was measured, and markers were placed at both ends; during the test, a net bag was used to catch all the threshing byproducts behind the shredder. After the test, maize kernels in the net bag were manually sorted and weighed to measure the carryover loss rate. Three random samples of the maize kernels from the grain bin were taken, as shown in Figure 9c. The impurities and broken kernels were manually sorted out from the samples, and the impurity rate and breakage rate were measured, with multiple measurements taken to obtain an average value. The testing process was divided into two groups: the first group did not make any adjustments to the threshing gap, keeping the adjustable lower sieve at the midpoint; the second group activated the threshing gap control system. The carryover loss rates of the two groups were compared, and the trend line is shown in Figure 10.

As can be seen from Table 5, the manual detection results for group 1 showed a carryover loss rate of 1.28%, a cleaning loss rate of 2.47%, an impurity rate of 0.59%, and a breakage rate of 2.51%. Group 2 had a carryover loss rate of 0.72%, a cleaning loss rate of 1.66%, an impurity rate of 0.62%, and a breakage rate of 2.45%. Comparing the threshing performance of the two groups, the carryover loss after control was reduced by 43.75%, and the cleaning loss rate decreased by 32.79%. The impurity rate increased by 5.08%, and the breakage rate decreased by 2.39%. The results indicate that while the impurity and breakage rates did not change significantly, the carryover loss rate and cleaning loss rate were reduced considerably. This study proposes that the threshing concave clearance control system can maintain grain loss within the ideal range for a period.



Figure 9. Field operation of harvester and manual collection; (a) field test of harvester material collection; (b) manual screening of lost grains; (c) grain bin contamination.

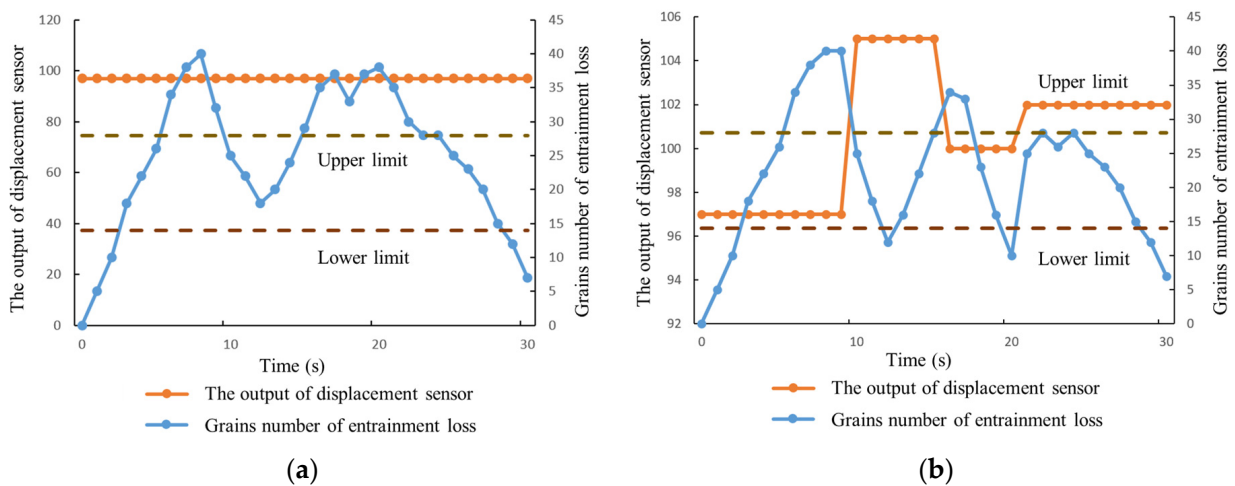


Figure 10. Comparison of loss variation trends before and after the opening of the threshing gap control system. (a). Turn off the control system; (b). Turn on the control system.

Table 5. Performance change rate before and after activating the threshing concave clearance control system.

Testing Number	Entrapment Loss Rate (%)	Cleaning Loss Rate (%)	Impurity Rate (%)	Breakage Rate (%)
Group 1	1.28	2.47	0.59	2.51
Group 2	0.72	1.66	0.62	2.45
Performance change rate	43.75	32.79	5.08	2.39

4. Conclusions

To address the challenges during complex field harvesting operations, where the threshing concave clearance structure of maize harvesters cannot be adjusted online based on real-time operational performance, this paper proposed an automatic control method for the threshing concave clearance of maize combine harvesters based on entrapment loss monitoring. This method achieved automatic control of the threshing concave clearance, effectively reduced grain loss, and provided important support for loss reduction in grain production and the intelligent harvesting equipment. The key conclusions are as follows:

- (1) A threshing gap adjustable concave sieve structure based on a crank-rocker mechanism was designed, and a mathematical model was established for the relationship between the threshing gap adjustment range and motor rotation angle. The adjustment range for the threshing gap was 15–47 mm, and the motor rotation angle was 0–48°. A carryover loss monitoring sensor based on piezoelectric ceramic-sensitive components was used, with signal processing calibration determining that a band-

pass filter frequency of 14–20 kHz can accurately identify maize kernels. An EDEM discrete element simulation model was established for maize ears and the mixture of extruded material, with simulation results identifying the optimal installation position for the loss sensor as the left rear of the concave sieve, with the minimum distance from the centerline of the sensitive plate to the threshing concave sieve being 58 mm and the installation angle of the sensor relative to the horizontal plane being 65°.

- (2) A maize threshing gap control method based on a fuzzy neural network PID control algorithm was proposed. Through Simulink simulation optimization, it was verified that this controller has superior performance with a fast response time. The designed maize threshing separation adjustment device was integrated with the carryover loss monitoring system on the harvester. Based on field harvesting tests at low, medium, and high speeds, combined with the set ideal carryover loss range, it was determined that the control device does not need to be activated at low speeds while activating the control system at medium speeds keeps the carryover loss within the set range, and at high speeds, the threshing gap should be set to the maximum adjustment plan. Finally, a comparison test of threshing performance before and after the control system was activated during medium-speed harvesting operations was designed, showing that the carryover loss rate was reduced by 43.75% after activating the control system, verifying the effectiveness of the control system and significantly reducing maize harvesting threshing losses. Future work will focus on real-time monitoring values for carryover and cleaning loss rates, impurity rates, and breakage rates, coordinating the control of threshing gap, sieve opening, fan speed, and other working parameters to comprehensively improve the threshing and cleaning performance of the harvester.

Author Contributions: Conceptualization, Y.Y. and C.F.; methodology, Y.Y.; software, M.Q.; formal analysis, Y.Y. and Q.W.; investigation, Y.Y.; data curation, X.Z. and L.C.; writing—original draft preparation, Y.Y.; writing—review and editing, C.F.; funding acquisition, Y.Y. and Y.C. All authors have read and agreed to the published version of the manuscript.

Funding: This study was supported by the Project of Faculty of Agricultural Engineering of Jiangsu University (NGXB20240202); 2023 Jiangsu Province Modern Agricultural Machinery Equipment and Technology Demonstration Promotion Project (NJ2023-04); Natural Science Foundation of Jiangsu Province (BK20230402); China Postdoctoral Science Foundation (2023M741723); and National Natural Science Foundation of China (52405277). Jiangsu Province Agricultural Science and Technology Independent Innovation Fund Project (CX(24)3030). The 2023 Hunan Province Smart Agricultural Machinery Equipment Innovation and Development Project ([2023]60).

Data Availability Statement: The original contributions presented in this study are included in the article. Further inquiries can be directed to the corresponding author.

Conflicts of Interest: Yi Cheng is employed by the Changzhou Changfa Heavy Industry Technology Co., Ltd. The remaining authors declare that the research was conducted in the absence of any commercial or financial relationships that could be construed as a potential conflicts of interest.

References

1. National Bureau of Statistics of China. *China Statistical Yearbook*; China Statistics Press: Beijing, China, 2023. Available online: https://www.stats.gov.cn/sj/zxfb/202312/t20231211_1945417.html (accessed on 2 December 2024).
2. Fan, C.; Zhang, D.; Yang, L.; Cui, T.; He, X.; Dong, J.; Zhao, H. Power consumption and performance of a maize thresher with automatic gap control based on feed rate monitoring. *Biosyst. Eng.* **2022**, *216*, 147–164. [\[CrossRef\]](#)
3. Cui, T.; Fan, C.L.; Zhang, D.X.; Yang, L.; LI, Y.B.; Zhao, H.H. Research progress of maize mechanized harvesting technology. *Trans. Chin. Soc. Agric. Mach.* **2019**, *50*, 1–13. [\[CrossRef\]](#)
4. Wang, K.R.; Li, S.K. Research progress on maize mechanical grain harvesting crushing rate. *Chin. Agric. Sci.* **2017**, *50*, 2018–2026. [\[CrossRef\]](#)

5. Li, W.; Hu, B.; Yan, Z.; Liu, S.; Shi, P.; Zhu, Y.; Li, H. The socio-ecological implications of shifting patterns of cropland use in northeast China. *J. Clean. Prod.* **2024**, *443*, 141050. [[CrossRef](#)]
6. Li, X.P.; Zhang, W.T.; Xu, S.D.; Du, Z.; Ma, Y.D.; Ma, F.L.; Liu, J. Low-damage maize threshing technology and maize threshing devices: A review of recent developments. *Agriculture* **2023**, *13*, 1006. [[CrossRef](#)]
7. Su, Y.; Xu, Y.; Cui, T.; Gao, X.J.; Xia, G.Y.; Li, Y.B.; Qiao, M.N.; Fan, H.F. A combined experimental and DEM approach to optimize the centrifugal maize breakage tester. *Powder Technol.* **2022**, *397*, 117008. [[CrossRef](#)]
8. Geng, A.J.; Yang, J.N.; Zhang, Z.L.; Zhang, J.; Li, R.Z. Discuss about the current situation and future of maize harvest machinery about domestic and abroad. *J. Agric. Mech. Res.* **2016**, *38*, 251–257.
9. Chen, M.; Jin, C.; Ni, Y.; Yang, T.; Zhang, G. Online field performance evaluation system of a grain combine harvester. *Comput. Electron. Agric.* **2022**, *198*, 107047. [[CrossRef](#)]
10. Li, X.; Du, Y.; Yao, L.; Wu, J.; Liu, L. Design and experiment of a broken maize kernel detection device based on the yolov4-tiny algorithm. *Agriculture* **2021**, *11*, 1238. [[CrossRef](#)]
11. Srison, W.; Chuan-Udom, S.; Saengprachatanarug, K. Design factors affecting losses and power consumption of an axial flow maize shelling unit. *Songklanakarin J. Sci. Technol.* **2016**, *38*, 591–598. [[CrossRef](#)]
12. Guan, Z.; Li, H.; Chen, X.; Mu, S.; Jiang, T.; Zhang, M.; Wu, C. Development of impurity-detection system for tracked rice combine harvester based on DEM and mask R-CNN. *Sensors* **2022**, *22*, 9550. [[CrossRef](#)] [[PubMed](#)]
13. Mahirah, J.; Kazuya, Y.; Munenori, M.; Naoshi, K.; Yuichi, O.; Tetsuhito, S.; Harshana, H.; Usman, A. Monitoring harvested paddy during combine harvesting using a machine vision-Double lighting system. *Eng. Agric. Environ. Food* **2017**, *10*, 140–149. [[CrossRef](#)]
14. Ferraretto, L.; Shaver, R.; Luck, B. Silage review: Recent advances and future technologies for whole-plant and fractionated maize silage harvesting. *J. Dairy Sci.* **2018**, *101*, 3937–3951. [[CrossRef](#)] [[PubMed](#)]
15. Saeng-ong, P.; Chuan-Udom, S.; Saengprachatanarak, K. Effects of guide vane inclination in axial shelling unit on maize shelling performance. *Kasetsart J.* **2015**, *49*, 761–771.
16. Zhu, X.L.; Chi, R.J.; Du, Y.F.; Deng, X.J.; Zhang, Z.; Dong, N.X. Design and experiment of intelligent control system for low loss threshing of high moisture content maize. *Trans. Chin. Soc. Agric. Mach.* **2021**, *52*, 9–18.
17. Geng, D.; Wang, Q.; Li, H.; He, Q.; Yue, D.; Ma, J.; Wang, Y.; Xu, H. Online detection technology for broken maize kernels based on deep learning. *Trans. Chin. Soc. Agric. Eng.* **2023**, *39*, 270–278. [[CrossRef](#)]
18. Fan, C.; Zhang, D.; Yang, L.; Cui, T.; He, X.; Qiao, M.; Sun, J.; Dong, J. A multi-parameter control method for maize threshing based on machine learning algorithm optimisation. *Biosyst. Eng.* **2023**, *236*, 212–223. [[CrossRef](#)]
19. Yu, Y.; Fu, H.; Yu, J. DEM-based simulation of the maize threshing process. *Adv. Powder Technol.* **2015**, *26*, 1400–1409. [[CrossRef](#)]
20. Yang, L.; Zhang, X.L.; Yaoming, L.; Liya, L.; Maolin, S. Modeling and control methods of a multi-parameter system for threshing and cleaning in grain combine harvesters. *Comput. Electron. Agric.* **2024**, *225*, 109251. [[CrossRef](#)]
21. Li, Y.; Xu, L.; Zhou, Y.; Li, B.; Liang, Z.; Li, Y. Effects of throughput and operating parameters on cleaning performance in air-and-screen cleaning unit: A computational and experimental study. *Comput. Electron. Agric.* **2018**, *152*, 141–148. [[CrossRef](#)]
22. Li, Y.; Xu, L.; Lv, L.; Shi, Y.; Yu, X. Study on modeling method of a multi-parameter control system for threshing and cleaning devices in the grain combine harvester. *Agriculture* **2022**, *12*, 1483. [[CrossRef](#)]
23. Omid, M.; Lashgari, M.; Mobli, H.; Alimardani, R.; Mohtasebi, S.; Hesamifard, R. Design of fuzzy logic control system incorporating human expert knowledge for combine harvester. *Expert Syst. Appl.* **2010**, *37*, 7080–7085. [[CrossRef](#)]
24. Ning, X.; Chen, J.; Li, Y.; Wang, K.; Wang, Y.; Wang, X. Kinetic model of combine harvester threshing system and simulation and experiment of speed control. *Trans. Chin. Soc. Agric. Eng.* **2015**, *31*, 25–34.
25. Zhang, Y. Mechanisms and Control Strategies Research on Threshing and Separating Quality of Combine Harvester. Doctoral Dissertation, China Agricultural University, Beijing, China, 2019.
26. Lian, Y. Study on Adaptive Control System of Operating Parameters for Threshing Device of Rice Wheat Combine Harvester. Master's Thesis, Jiangsu University, Zhenjiang, China, 2020.
27. Zhu, X.; Chi, R.; Du, Y.; Ban, C.; Ma, Y.; Huang, X. Design of Hardware in loop simulation platform for intelligent control system of maize kernel harvester. *Trans. Chin. Soc. Agric. Mach.* **2022**, *53*, 114–122.
28. Jigang, H.; Jie, W.; Hui, F. An anti-windup self-tuning fuzzy PID controller for speed control of brushless DC motor. *Autom. Časopis Autom. Mjer. Elektron. Računarstvo I Komun.* **2017**, *58*, 321–335. [[CrossRef](#)]
29. Lin, F.J.; Wai, R.J.; Lee, C.C. Fuzzy neural network position controller for ultrasonic motor drive using push-pull DC-DC converter. *IEE Proc.-Control Theory Appl.* **1999**, *146*, 99–107. [[CrossRef](#)]
30. Wang, Y. Research on Water Injection Flow Control Strategy Based on Fuzzy Neural Network PID. Master's Thesis, Harbin University of Science and Technology, Harbin, China, 2020.
31. Fan, C. Research on Intelligent Optimization PID Controller Based on Fuzzy Neural Network. Master's Thesis, Beijing University of Chemical Technology, Beijing, China, 2009.

32. Lachuga, Y.F.; Bur'yanov, A.I.; Pakhomov, V.I.; Chervyakov, I.V. Adaptation of threshing devices to physical and mechanical characteristics of harvested crops. *Russ. Agric. Sci.* **2020**, *46*, 198–201. [[CrossRef](#)]
33. Bakharev, D.; Pastukhov, A.; Volvak, S.; Kovalev, S. Study of seed maize threshing process. *Eng. Rural Dev.* **2020**, *19*, 1036–1041.

Disclaimer/Publisher's Note: The statements, opinions and data contained in all publications are solely those of the individual author(s) and contributor(s) and not of MDPI and/or the editor(s). MDPI and/or the editor(s) disclaim responsibility for any injury to people or property resulting from any ideas, methods, instructions or products referred to in the content.